

Reconnexion of vortex and magnetic tubes subject to an imposed strain: An approach by perturbation expansion

This article has been downloaded from IOPscience. Please scroll down to see the full text article.

2005 Fluid Dyn. Res. 36 333

(<http://iopscience.iop.org/1873-7005/36/4-6/A14>)

View [the table of contents for this issue](#), or go to the [journal homepage](#) for more

Download details:

IP Address: 131.111.17.180

The article was downloaded on 15/09/2013 at 22:53

Please note that [terms and conditions apply](#).



ELSEVIER

Available online at www.sciencedirect.com

SCIENCE @ DIRECT®

Fluid Dynamics Research 36 (2005) 333–356

FLUID DYNAMICS
RESEARCH

Reconnexion of vortex and magnetic tubes subject to an imposed strain: An approach by perturbation expansion

Y. Hattori^{a,*}, H.K. Moffatt^b^a*Division of Computer Aided Science, Kyushu Institute of Technology, Tobata, Kitakyushu 804-8550, Japan*^b*Department of Applied Mathematics and Theoretical Physics, Wilberforce Road, Cambridge CB3 0WA, UK*

Received 19 March 2004; received in revised form 20 January 2005; accepted 29 January 2005

Communicated by S. Kida

Abstract

The viscous interaction of two weakly curved and oppositely directed vortex tubes of flattened cross-section driven together by an imposed uniform strain is considered using a perturbation technique. The evolution of the cross-sectional vorticity distribution is computed, and the rate of reconnexion, as indicated by the decrease of circulation of each tube at the plane of symmetry, is obtained for various values of the Reynolds number and of the (small) aspect ratio of the tubes. Attention is focused particularly on the nonlinear effect of convection by the velocity field induced by the vortices. A similar technique is applied to the problem of reconnexion of magnetic flux tubes, for which the nonlinear effect is different, being that associated with the Lorentz force distribution.

© 2005 Published by The Japan Society of Fluid Mechanics and Elsevier B.V. All rights reserved.

Keywords: Vortex reconnexion; Magnetic reconnexion; Perturbation expansion; Uniform strain field

1. Introduction

Vortex reconnexion is a process of fundamental importance in both laminar and turbulent flow. It occurs as a result of viscous diffusion when two or more vortex tubes come into close proximity, either through their own self-induced motion, or as the result of a strain field induced by remote vorticity (for a review, see [Kida and Takaoka, 1994](#)).

* Corresponding author. Tel./fax: +81 93 884 3410.

E-mail address: hattori@mns.kyutech.ac.jp (Y. Hattori).

The process can involve intense vortex stretching and has attracted great interest in the context of the ‘finite-time singularity problem’ for the Euler and/or Navier–Stokes equations (see, for example, the book “Tubes, Sheets and Singularities in Fluid Dynamics” (Bajer and Moffatt, 2002)). In this context, the pioneering work of Pelz (1997, 2001) deserves particular mention. Pelz used vortex filament techniques, exploiting the symmetries of an initial highly symmetric array of vortex tubes propagating towards the planes of symmetry, to reveal an apparently self-similar evolution towards a point singularity at finite time; this was for the Euler equations, but in a real fluid, viscous reconnection at or near this incipient singularity would appear to be inevitable.

Among the analytical approaches to the vortex reconnection problem, there is a family of exact solutions of the Navier–Stokes equations (Kambe, 1983) which can serve as a starting point for a perturbative approach. Kambe, described mutual annihilation of two vortex sheets driven towards each other by an imposed uniform strain field. A variant on this, involving the viscous interaction of straight jets, again driven together by an imposed uniform strain, was analysed by Takaoka (1991). In both cases, the configuration involved a vorticity or velocity field parallel to planes $x = \text{const.}$, and depending only on one or two of the Cartesian coordinates, and nonlinear effects associated with convection of vorticity by its own self-induced velocity field were consequently absent.

If we allow weak variation of Kambe’s (1983) field in the y - and z -directions, then we are considering a configuration like that sketched in Fig. 1, in which two flat, weakly-curved, oppositely-directed vortex tubes are driven together by a strain field of the form

$$U_0 = (\alpha x, \beta y, \gamma z), \quad (1)$$

where

$$\alpha + \beta + \gamma = 0, \quad \alpha < 0, \quad \beta > 0. \quad (2)$$

The tubes are ‘flat’ in the sense that the field variation in the z -direction is slow compared with that in the x -direction; and the vortex tubes are weakly curved in the y -direction. These conditions are clearly compatible with, and indeed reinforced by, the strain field (1),(2). The annihilation process identified by Kambe will now act more rapidly near the plane $y = 0$ and a genuine reconnection of vortex lines will occur initially in this neighbourhood. At the same time, the weak z -variation results in a nontrivial induced velocity field which affects the reconnection process. We shall develop a perturbation expansion, exploiting the assumed weak variation in the y - and z -directions, thus taking some account of the nonlinearity associated with this process. We shall find that it is the z -dependence, leading to counter-rotation of the two vortices, that first influences the reconnection process.

Reconnection of magnetic flux tubes may be similarly treated, and the process is in fact identical at the lowest order when variation in the y - and z -directions is suppressed. At higher orders however, differences appear, due to the different character of the nonlinear Lorentz force as compared with the nonlinear self-induced convection of vorticity. If the tubes of Fig. 1 are magnetic flux tubes, then the Lorentz force appears through the Maxwell tension in the curved lines of force which is believed to accelerate reconnection once this process has been initiated. Magnetic reconnection plays a key role in the theory of solar flares and coronal heating (see Priest and Forbes, 2000 for an extensive review). In most previous studies, steady configurations of flow and field have been analysed, and reconnection has been inferred from inflow and outflow conditions (Craig and Henton, 1995; Priest et al., 2000). In this paper, we study unsteady reconnection, in which the change of field topology that is necessarily associated with this process is evident.

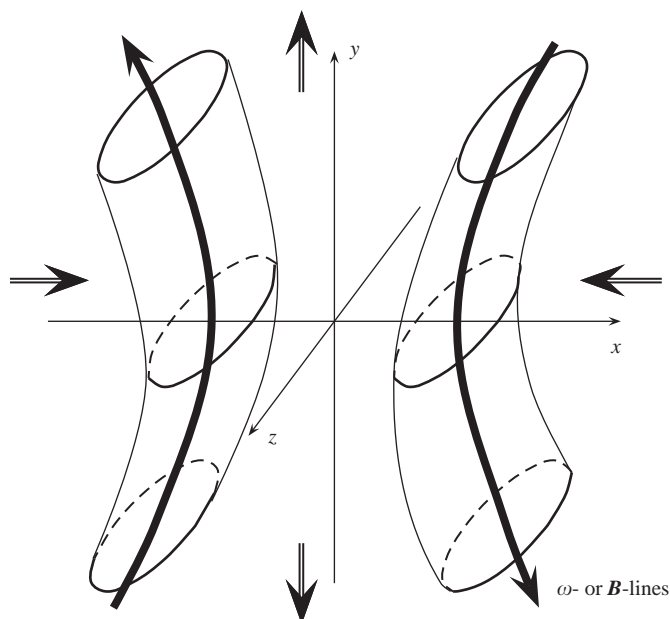


Fig. 1. Reconnection of flat tubes under a strain field. Schematic diagram. The tubes are flat in the sense that their cross-sectional scale is much larger in the z -direction than in the x -direction.

The process of ‘accelerated ohmic diffusion’ under the action of two-dimensional uniform strain was described by Moffatt (1978); this is somewhat analogous to Kambe’s (1983) model for vorticity annihilation. An unsteady model of magnetic reconnection (as in Fig. 1, but with no variation in the z -direction), has been proposed more recently by Moffatt and Hunt (2002); in this model, strong variation in the x -direction and weak variation in the y -direction conspire to allow the use of boundary-layer techniques. Nonlinearity, as indicated above, is associated primarily with curvature of the magnetic lines of force; thus, unlike the case of vortex reconnection, field variation in the y -direction is of primary importance, and variation in the z -direction has negligible effect. In Section 3 below, we adopt the alternative perturbation approach, focusing on the differences between the behaviour of vortex tubes and magnetic flux tubes as revealed by this analysis.

Perturbation theory of the type presented here has an extremely limited range of validity in the parameter space, and cannot possibly describe the sort of explosive reconnection events associated either with intense vortex stretching or with ‘fast’ magnetic reconnection on the Alfvén time-scale. Such behaviour can at present be captured only by full-scale numerical simulation. Perturbation theory may nevertheless play a useful complementary role in providing an indication of some of the physical processes that underlie reconnection mechanisms.

2. Vortex reconnection

2.1. Perturbation approach

We first consider vortex reconnection of flat tubes under a strain field. The initial vortex tubes are assumed to be almost parallel to the y -axis and slightly curved away from it as $|y|$ becomes large

(Fig. 1). The tube sections are ellipses whose minor and major axes in the plane $y = 0$ are parallel to the x - and z -axes, respectively, and assumed to be in a ratio of $O(\varepsilon)$, where $0 < \varepsilon \ll 1$. We assume further that the field variation in both y and z is $O(\varepsilon)$; we thus suppose that

$$\mathbf{U} = \mathbf{U}_0 + \mathbf{u}, \quad \mathbf{u} = \mathbf{u}(x, \tilde{y}, \tilde{z}), \quad \tilde{y} = \varepsilon y, \quad \tilde{z} = \varepsilon z, \quad 0 < \varepsilon \ll 1. \tag{3}$$

In the following the strain rates α, β, γ are assumed constant for simplicity; the results may be easily generalised to the case of time-dependent strain rates (see Appendix A). We consider the following type of flow:

$$\mathbf{u} = \begin{pmatrix} u \\ v \\ w \end{pmatrix} = \begin{pmatrix} 0 \\ 0 \\ w^{(0)} \end{pmatrix} + \varepsilon \begin{pmatrix} u^{(1)} \\ v^{(1)} \\ w^{(1)} \end{pmatrix} + \varepsilon^2 \begin{pmatrix} u^{(2)} \\ v^{(2)} \\ w^{(2)} \end{pmatrix} + \dots$$

Then the vorticity field is

$$\boldsymbol{\omega} = \begin{pmatrix} 0 \\ -\frac{\partial w^{(0)}}{\partial x} \\ 0 \end{pmatrix} + \varepsilon \begin{pmatrix} \frac{\partial w^{(0)}}{\partial \tilde{y}} \\ -\frac{\partial w^{(1)}}{\partial x} \\ \frac{\partial v^{(1)}}{\partial x} \end{pmatrix} + \varepsilon^2 \begin{pmatrix} \frac{\partial w^{(1)}}{\partial \tilde{y}} - \frac{\partial v^{(1)}}{\partial \tilde{z}} \\ -\frac{\partial w^{(2)}}{\partial x} + \frac{\partial u^{(1)}}{\partial \tilde{z}} \\ \frac{\partial v^{(2)}}{\partial x} - \frac{\partial u^{(1)}}{\partial \tilde{y}} \end{pmatrix} + \dots$$

Substituting these expansions in the vorticity equation

$$\frac{\partial \boldsymbol{\omega}}{\partial t} + \mathbf{U} \cdot \nabla \boldsymbol{\omega} = \boldsymbol{\omega} \cdot \nabla \mathbf{U} + \nu \nabla^2 \boldsymbol{\omega} \tag{4}$$

and the incompressibility condition

$$\nabla \cdot \mathbf{U} = 0 \tag{5}$$

gives equations at each order $O(\varepsilon^n)$. We restrict attention to situations for which

$$\mathbf{u}^{(n)}, \quad \text{is bounded, as } |x| \rightarrow \infty. \tag{6}$$

Note here that if the initial condition is independent of \tilde{z} , then u and v remain identically zero for all $t > 0$, and w is convected (by \mathbf{U} and diffused, like a passive scalar). It is only \tilde{z} -variation that leads to nonlinear 'self-advection' effects.

2.2. Derivation of equations at each order

The equations at each order are detailed in Appendix A. Here we just derive the leading-order equations to indicate the procedure. At this leading order, the x - and z -components of the vorticity equation are trivial. The y -component becomes

$$(L_\nu - \beta) \frac{\partial w^{(0)}}{\partial x} = 0, \tag{7}$$

where the operator L_ν , which depends on diffusivity ν , is defined by

$$L_\nu = \frac{\partial}{\partial t} + \alpha x \frac{\partial}{\partial x} + \beta \tilde{y} \frac{\partial}{\partial \tilde{y}} + \gamma \tilde{z} \frac{\partial}{\partial \tilde{z}} - \nu \frac{\partial^2}{\partial x^2}, \tag{8}$$

this integrates with the boundary condition (6), to give

$$(L_v + \gamma)w^{(0)} = 0. \tag{9}$$

The incompressibility condition is trivially satisfied.

At each order, equations similar to Eq. (9) are transformed into one-dimensional diffusion equations of the form

$$\left(\frac{\partial}{\partial t} - v e^{-2\alpha t} \frac{\partial^2}{\partial X^2}\right) f = s, \tag{10}$$

where $X = e^{-\alpha t} x$ (see Appendix A for the details). The solution is

$$f(X, t) = \int f(X', 0)G(X - X', t) dX' + \int \int s(X', t')G(X - X', t - t') dX' dt', \tag{11}$$

where

$$G(X, t) = \frac{1}{\sqrt{4\pi v D_x(t)}} \exp\left[-\frac{X^2}{4v D_x(t)}\right] \tag{12}$$

with

$$D_x(t) = \int_0^t e^{-2\alpha s} ds = \frac{1}{2\alpha}(1 - e^{-2\alpha t}). \tag{13}$$

2.3. Example

For example, let us take the following initial vorticity distribution (at leading order):

$$\begin{aligned} \omega_y^{(0)}(x, \tilde{y}, \tilde{z}, 0) = & -\frac{W_0}{\sqrt{\pi}a} \left[\exp\left(-\frac{\left\{x + \sqrt{k^2\tilde{y}^2 + X_0^2}\right\}^2}{a^2}\right) \right. \\ & \left. - \exp\left(-\frac{\left\{x - \sqrt{k^2\tilde{y}^2 + X_0^2}\right\}^2}{a^2}\right) \right] \exp\left(-\frac{\tilde{z}^2}{a^2}\right). \end{aligned} \tag{14}$$

Here, the initial vorticity is centred on the hyperbolic sheets $x^2 - k^2\tilde{y}^2 = X_0^2$ as sketched in Fig. 1 (note that the x -component of vorticity is $O(\epsilon)$). This initial condition is separable in \tilde{z} , which simplifies the analysis. It turns out that all variables are expressed by functions separable in \tilde{z} so that we can obtain fields in the xz -plane by solving a single set of one-dimensional diffusion equations. Then $w^{(0)}$ and $u^{(1)}$ (for $t > 0$) can be found by explicit integration. The remaining variables may be found by numerical integration of equations of the form (A.27); we used the compact scheme of Lele (1992) for spatial derivatives and a fourth-order Runge–Kutta method for time evolution. The case considered by Kambe (1983) is recovered by taking $\epsilon = 0$ (and $k = 0$).

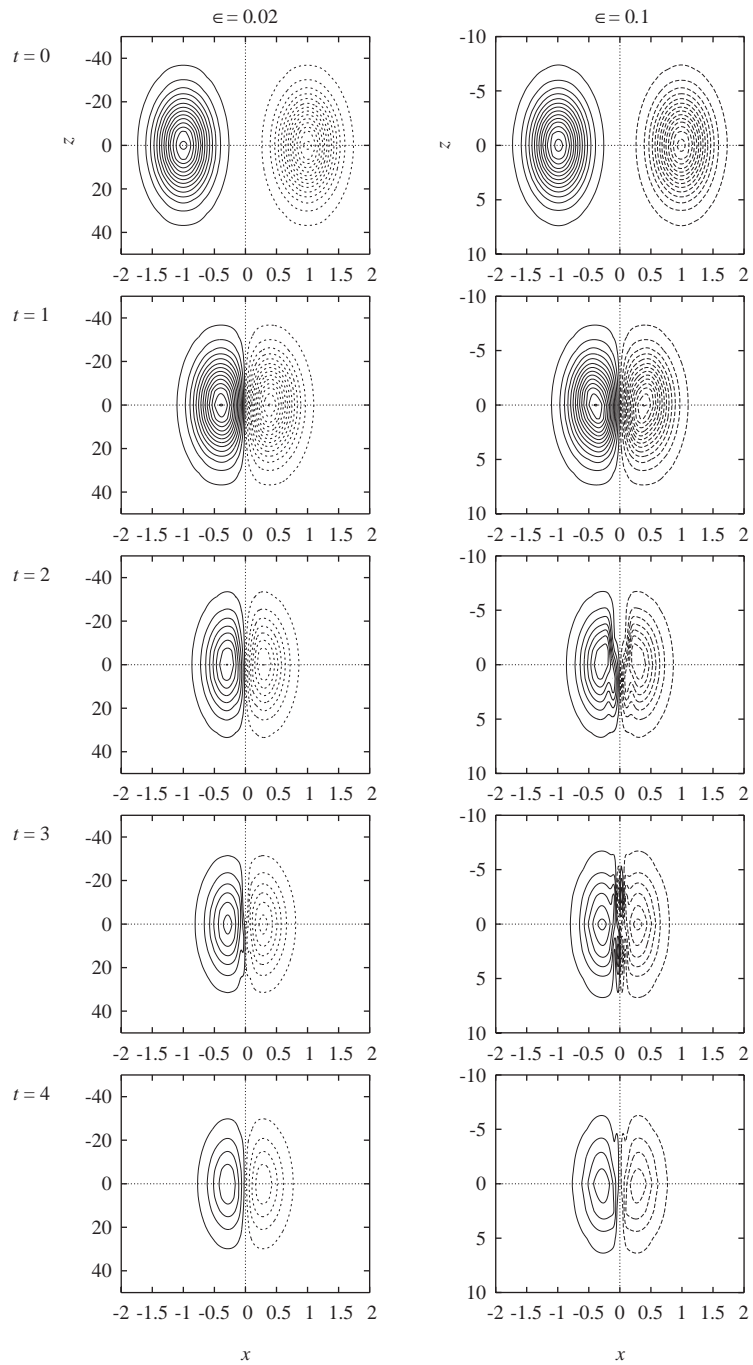


Fig. 2. Vortex reconnection. Contours of ω_y in $y = 0$. (Left) $\epsilon = 0.02$, (right) $\epsilon = 0.1$.

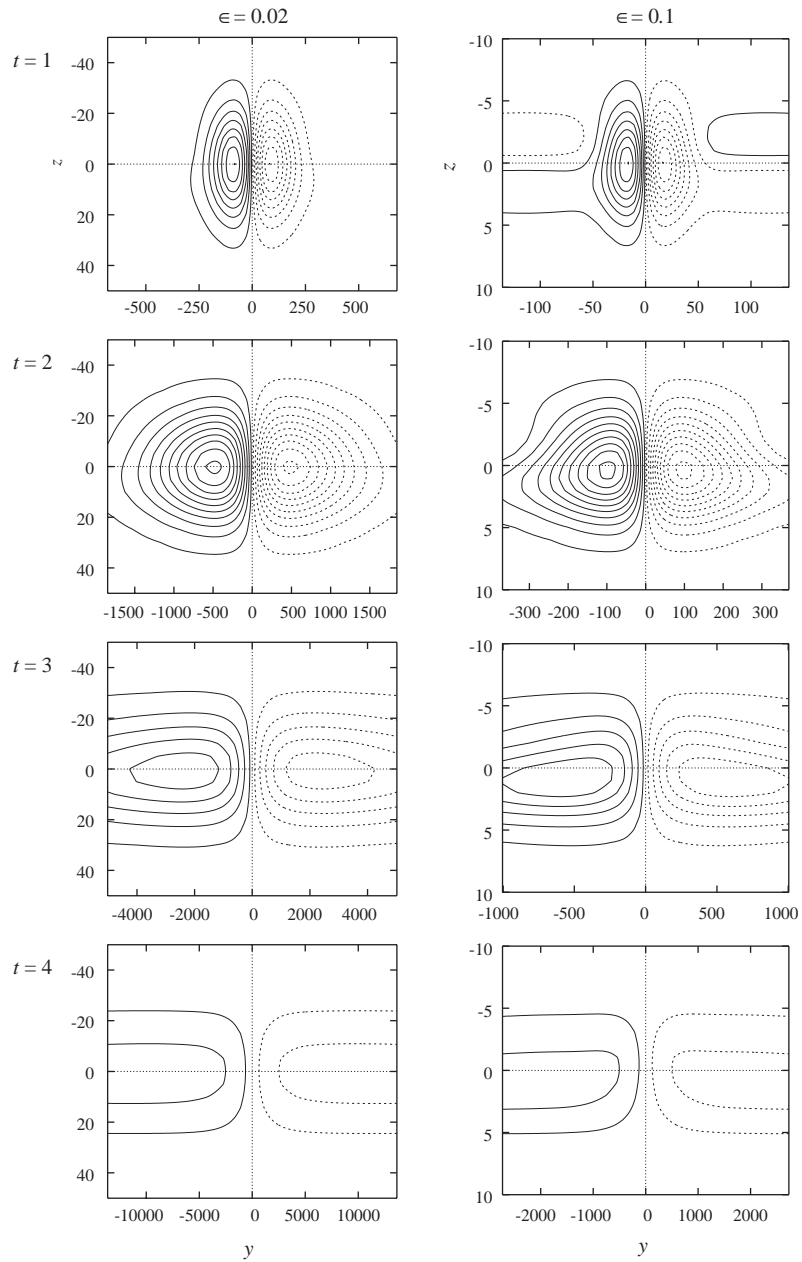


Fig. 3. Vortex reconnection. Contours of ω_x in $x = 0$. (Left) $\varepsilon = 0.02$, (right) $\varepsilon = 0.1$.

The motion of the tubes is shown by the vorticity contours in Figs. 2 and 3. Fig. 2 shows contours of ω_y , which is the *original* field before reconnection, in the xz -plane ($y = 0$); Fig. 3 shows contours of ω_x , which is the *reconnected* field, in the yz -plane ($x = 0$). Note that the aspect ratio is far from unity in these

figures. The strain rates are taken as

$$\alpha = -s_0, \quad \beta = s_0, \quad \gamma = 0,$$

where s_0 is a positive constant. The dimensionless parameters of the problem are set to the values

$$a^* = \frac{a}{X_0} = 0.4, \quad \mu = \frac{W_0}{s_0 X_0} = 0.2, \quad Re = \frac{W_0 a}{\nu} = 100, \quad k = 1, \quad \varepsilon = 0.02, 0.1.$$

Both components of vorticity are calculated upto $O(\varepsilon^2)$. In Fig. 2, the tubes, whose sections are ellipses at $t = 0$, are convected towards the z -axis where the vortex lines reconnect, a process that becomes increasingly visible for $t \geq 1$. As reconnection proceeds, the magnitude of ω_y decreases (for $t \geq 2$). The points of extremal vorticity effectively come to rest for $t \gtrsim 1$ as a layer of thickness $\sim \sqrt{\nu/s_0}$ forms along $x = 0$. At $t = 1$ for $\varepsilon = 0.1$ we observe that the tube sections have been slightly rotated under the action of the self-induced velocity, the right tube clockwise, and the left tube anticlockwise. For $\varepsilon = 0.02$, the tube sections are almost symmetric with respect to the x -axis, but slight rotation is visible at $t = 3$. This self-induced rotation accelerates reconnection in $z > 0$. At $t = 3$ for $\varepsilon = 0.1$ vorticity of opposite sign appears in the half planes $x > 0$ and $x < 0$. This may be an artifact of the perturbation expansion suggesting that, as discussed below, the domain of convergence of the ε -expansion may be quite narrow in the parameter space.

The reconnected field (represented by the component ω_x) shown in Fig. 3 can be interpreted as a cross-section of *bridges*, in the terminology of Melander and Hussain (1988). The reconnected field is seen to move rapidly away from the plane $y = 0$; (note that the aspect ratio of the frame changes with time since we choose a fixed range for $Y = ye^{s_0 t}$). This rapid motion is roughly proportional to $e^{(-\alpha+\beta)t} = e^{2s_0 t}$. It is a consequence of a dual effect of the strain: compression in x makes the tubes contact first at the origin and then successively at larger Y ; and stretching in y also expands the reconnection region. The field is stronger in $z > 0$ than in $z < 0$. This is due to the self-induced rotation observed in Fig. 2; in other words, it is a weakly nonlinear effect of $O(\varepsilon^2)$. The weak positive/negative vorticity which appears in the positive/negative y -region at $t = 1$ is probably an artifact of the expansion.

It is difficult to determine the region of convergence of the present perturbation expansion. However, a rough estimate is given by the ratio of norm of the vorticity component in an appropriate function space. We calculate the following ratio:

$$R^{(i)} = \frac{\|\omega_y^{(i)}\|}{\|\omega_y^{(i+1)}\|}, \quad \|f\|^2 = \int \int f(x, 0, z) dx dz. \tag{15}$$

The present expansion is expected to converge if

$$\varepsilon < \varepsilon_c = \limsup_{i \rightarrow \infty} R^{(i)}. \tag{16}$$

Although $R^{(i)}$ is available only for $i = 0$ and 1, it may still give a reasonable estimate of the region of convergence.

Fig. 4 shows time evolution of $R^{(0)}$, $R^{(1)}$ and $\sqrt{R^{(0)}R^{(1)}}$. The case $\mu = 1$, in which strain is relatively weaker than in $\mu = 0.2$, is also included here for comparison. For $\mu = 0.2$, the minima of $R^{(0)}$ and $R^{(1)}$ are about 0.42 (at $t = 2.9$) and 0.66 (at $t = 3.7$), respectively. Thus ε_c is expected to be $O(10^{-1})$. For the

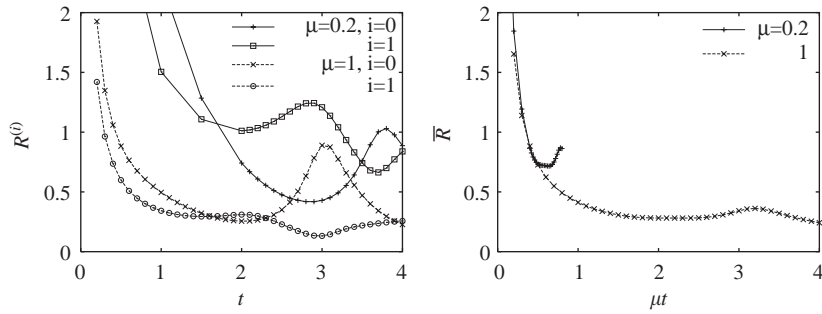


Fig. 4. Time evolution of (Left) $R^{(i)}$ and (right) $\bar{R} = \sqrt{R^{(0)}R^{(1)}}$.

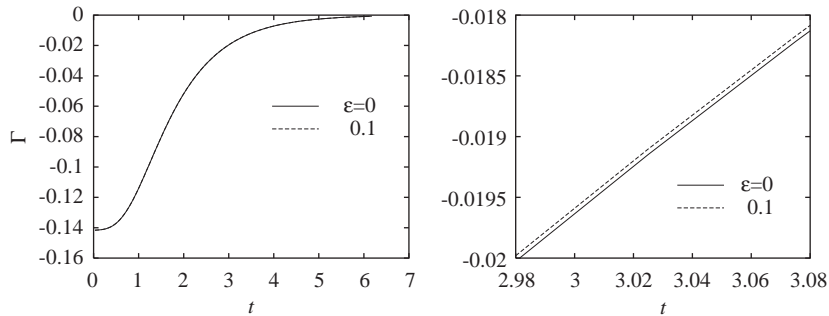


Fig. 5. Time evolution of circulation of one tube. $\varepsilon = 0, 0.1$. Curves for $2.98 < t < 3.08$ are magnified on the right.

weaker strain $\mu = 1$, however, $R^{(1)}$ is lower than 0.3 for $t > 1.4$ and the minimum is about 0.13 (at $t = 3$). Thus the range of convergence is much narrower for $\mu = 1$. One of the mechanisms which determine the range of convergence is deduced from the right figure, where the geometric mean of $R^{(0)}$ and $R^{(1)}$, $\bar{R} = \sqrt{R^{(0)}R^{(1)}} = \sqrt{\|\omega_y^{(0)}\|/\|\omega_y^{(2)}\|}$, is shown against a scaled time μt . The two curves coincide up to $\mu t \sim 0.4$; \bar{R} decreases as higher-order terms grow with time. For $\mu = 0.2$, \bar{R} stops decreasing around $\mu t \sim 0.4$ as strain forces the two tubes to reconnect. On the other hand \bar{R} keeps decreasing until $\mu t \sim 2$ when the two tubes start reconnecting. In other words, for the stronger strain (smaller μ), the region of convergence is larger since there is insufficient time for nonlinearity to grow.

The ‘artifacts’ observed in Figs. 2 and 3 are sometimes encountered when one truncates perturbation expansions. For example, Fukumoto and Moffatt (2000) obtained the vorticity distribution of a viscous vortex ring by perturbation expansion upto second order in the ratio of core- to ring-radius; a region of opposite-signed vorticity could not be avoided for rather small value of the expansion parameter. However, the expansion gives quite accurate values of global quantities like the speed of the vortex ring. The present expansion is similarly expected to give reasonably accurate results for the range of ε estimated as above.

Fig. 5 shows the evolution of the circulation of one tube evaluated in the xz -plane

$$\Gamma(t) = \int_{-\infty}^{\infty} dz \int_0^{\infty} dx \omega_y, \tag{17}$$

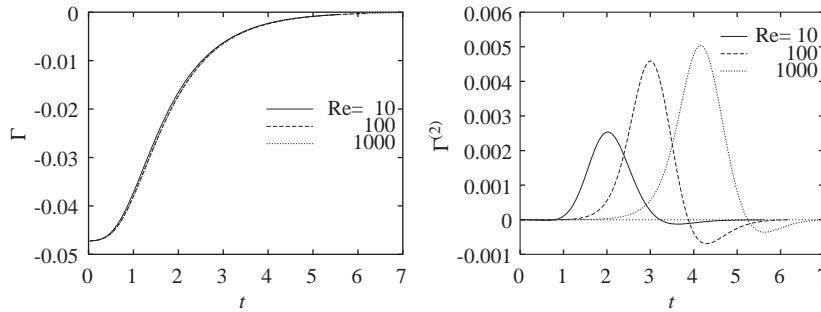


Fig. 6. Time evolution of circulation of one tube. Reynolds number dependence. $\epsilon = 0.1$. (Left) total circulation $\Gamma = \Gamma^{(0)} + \epsilon^2 \Gamma^{(2)}$, (right) second-order term $\Gamma^{(2)}$.

which provides a measure of the rate of vortex reconnection, for $\epsilon = 0$ and 0.1 , other parameters being unchanged. Note that $\epsilon = 0$ corresponds to annihilation of vortex sheets. The difference between the two cases is small, implying that nonlinearity here has a small effect on the overall rate of reconnection. In fact, Γ has the expansion

$$\Gamma(t) = \Gamma^{(0)}(t) + \epsilon^2 \Gamma^{(2)}(t) + O(\epsilon^4), \tag{18}$$

in which the $O(\epsilon)$ term vanishes.

The evolution of Γ and $\Gamma^{(2)}$ for $\epsilon = 0.1$ and $Re = 10, 100, 1000$ is shown in Fig. 6; other parameters being unchanged. The total circulation Γ does not vary much with Re . It should be noted that the second-order effect accelerates reconnection. This second-order effect becomes larger and appears at later time as Re becomes larger; this is probably because the ‘reconnection layer’ located around the z -axis becomes thinner as Re becomes larger so that strong vorticity persists for a longer time.

The influence of γ , the strain rate in the z -direction, is also shown. In Fig. 7 the second-order circulation $\Gamma^{(2)}$ is shown for three values of γ : $-0.2s_0, 0, 0.5s_0$; α is fixed: $\alpha = -s_0, \beta = s_0 - \gamma$. Here, the positive value $0.5s_0$ was chosen to give an imposed strain that is symmetric in the yz -plane. The negative value ($-0.2s_0$) was set to be small in magnitude since larger values (e.g. $\gamma = -0.5s_0$) need more severe conditions for convergence of the ϵ -expansion. We see that compression in z ($\gamma < 0$) increases the acceleration of reconnection, while stretching ($\gamma > 0$) decreases it. This is because the self-induced rotation is enhanced for $\gamma < 0$ and diminished for $\gamma > 0$ since the cross section is compressed or stretched, respectively (Fig. 8); the factor $e^{-2\gamma t}$ in Eqs. (A.17) and (A.19) is responsible for this effect.

3. Magnetic reconnection

3.1. Perturbation approach

For magnetic reconnection we consider the same problem as for vortex reconnection, simply replacing the vorticity field $\omega_y^{(0)}$ in the initial condition by a magnetic field $B_y^{(0)}$; thus, we set

$$\mathbf{U} = \mathbf{U}(x, \tilde{y}, \tilde{z}), \quad \mathbf{B} = \mathbf{B}(x, \tilde{y}, \tilde{z}), \quad \tilde{y} = \epsilon y, \quad \tilde{z} = \epsilon z, \quad 0 < \epsilon \ll 1, \tag{19}$$

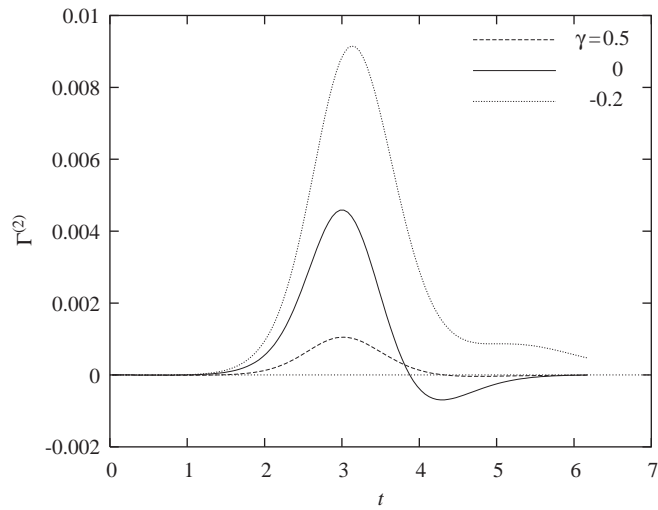


Fig. 7. Time evolution of the second-order circulation $\Gamma^{(2)}$ of one tube. Dependence on γ .

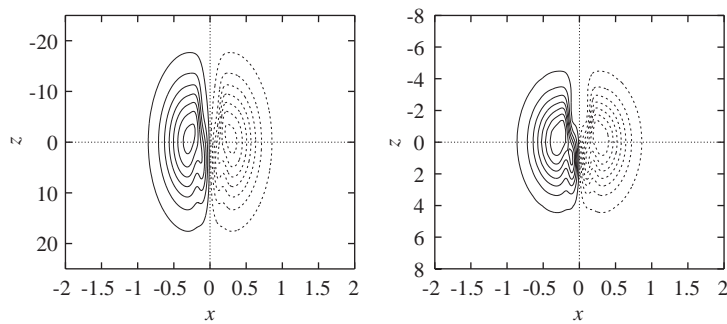


Fig. 8. Vortex reconnection. Dependence on γ . Contours of ω_y in $y = 0$. $\varepsilon = 0.1$, $t = 2$. (Left) $\gamma = 0.5s_0$, (right) $\gamma = -0.2s_0$.

where the derivatives with respect to x , \tilde{y} , \tilde{z} are of the same order of magnitude. We consider the following type of flow and field:

$$U = \begin{pmatrix} \alpha x \\ \beta y \\ \gamma z \end{pmatrix} + \mathbf{u}, \quad \mathbf{u} = \varepsilon \mathbf{u}^{(1)} + \varepsilon^2 \mathbf{u}^{(2)} + \dots, \tag{20}$$

$$\mathbf{B} = \begin{pmatrix} B_x \\ B_y \\ B_z \end{pmatrix} = \begin{pmatrix} 0 \\ B_y^{(0)} \\ 0 \end{pmatrix} + \varepsilon \begin{pmatrix} B_x^{(1)} \\ B_y^{(1)} \\ B_z^{(1)} \end{pmatrix} + \dots. \tag{21}$$

The MHD equations are

$$\frac{\partial \mathbf{U}}{\partial t} + (\mathbf{U} \cdot \nabla) \mathbf{U} = -\nabla p_* + (\mathbf{B} \cdot \nabla) \mathbf{B} + \nu \nabla^2 \mathbf{U}, \tag{22}$$

$$\frac{\partial \mathbf{B}}{\partial t} + (\mathbf{U} \cdot \nabla) \mathbf{B} = (\mathbf{B} \cdot \nabla) \mathbf{U} + \eta \nabla^2 \mathbf{B}, \tag{23}$$

$$\nabla \cdot \mathbf{U} = 0, \quad \nabla \cdot \mathbf{B} = 0, \tag{24}$$

where p_* is the total pressure and ν and η are non-dimensionalized coefficients of kinematic viscosity and magnetic diffusivity, respectively. We assume $B_z^{(1)} = 0$ initially which implies $B_z^{(1)} = 0$ for all t .

3.2. Remarks on derivation of equations at each order

The procedure for obtaining equations at each order is similar to that used for vortex reconnection, and the various evolution equations may be transformed to one-dimensional diffusion equations (see Appendix B for details). It should be noted that by induction we have

$$u^{(2n-1)} = v^{(2n)} = w^{(2n)} = 0, \tag{25}$$

$$B_x^{(2n)} = B_y^{(2n-1)} = B_z^{(2n-1)} = 0, \tag{26}$$

$$p_*^{(2n-1)} = 0, \tag{27}$$

so that the fields are

$$\mathbf{u} = \varepsilon \begin{pmatrix} 0 \\ v^{(1)} \\ 0 \end{pmatrix} + \varepsilon^2 \begin{pmatrix} u^{(2)} \\ 0 \\ 0 \end{pmatrix} + \varepsilon^3 \begin{pmatrix} 0 \\ v^{(3)} \\ w^{(3)} \end{pmatrix} + \dots, \tag{28}$$

$$\mathbf{B} = \begin{pmatrix} 0 \\ B_y^{(0)} \\ 0 \end{pmatrix} + \varepsilon \begin{pmatrix} B_x^{(1)} \\ 0 \\ 0 \end{pmatrix} + \varepsilon^2 \begin{pmatrix} 0 \\ B_y^{(2)} \\ 0 \end{pmatrix} + \varepsilon^3 \begin{pmatrix} B_x^{(3)} \\ 0 \\ 0 \end{pmatrix} + \varepsilon^4 \begin{pmatrix} 0 \\ B_y^{(4)} \\ B_z^{(4)} \end{pmatrix} + \dots. \tag{29}$$

This difference from the hydrodynamic case is remarkable, in view of the fact that the vorticity equation in the hydrodynamic case has the same structure as the induction equation. This is due to the difference in nonlinear coupling in the hydrodynamic and magnetic cases: in the hydrodynamic case, the nonlinear terms of the vorticity equation are essentially second order in \mathbf{u} , while in the magnetic case the nonlinear terms of the induction equation are *linear* in \mathbf{B} . Since $O(1)$ velocity is absent apart from the applied strain, it takes two steps, one in the momentum equation (coming from the Lorentz force $\mathbf{B} \cdot \nabla \mathbf{B}$) and the other in the induction equation, for nonlinear effects to feed back to the reconnection process.

Note also that w and B_z are zero up to $O(\varepsilon^2)$ and $O(\varepsilon^3)$, respectively. Up to $O(\varepsilon^2)$, the z -components of velocity field and magnetic field are zero and the only term that includes z -differentiation is the dissipation term in the equation of $B_y^{(2)}$; the problem is almost two-dimensional by virtue of setting $B_z^{(1)} = 0$ initially. Thus we are justified in restricting attention to the two-dimensional problem in the following.

3.3. Example: two-dimensional case

As in Moffatt and Hunt (2002), we take

$$B_y^{(0)}(x, \tilde{y}; 0) = -B_0 \left[\exp\left(-\frac{\left\{x + \sqrt{k^2 \tilde{y}^2 + X_0^2}\right\}^2}{a^2}\right) - \exp\left(-\frac{\left\{x - \sqrt{k^2 \tilde{y}^2 + X_0^2}\right\}^2}{a^2}\right) \right]. \quad (30)$$

For $t > 0$, we have explicit solutions for $B_y^{(0)}$, $B_x^{(1)}$. The rest are obtained numerically.

Fig. 9 shows time evolution of magnetic lines of force. Since contours of magnetic potential A_z ($B_x = \partial_y A_z$, $B_y = -\partial_x A_z$) are drawn with a constant increment, the density of lines is proportional to the magnitude of the magnetic fields. Note again that the range of x and y vary with time as imposed strain stretches the field lines significantly. Starting from the initial condition, the magnetic lines are convected to the y -axis ($t = 1$); they reconnect on the y -axis ($t = 2$ and 3) and are convected away from the origin ($t = 4$). Nonlinear effects are hardly visible in this figure in spite of the rather large value of $\varepsilon = 0.5$; this suggests that the range of convergence is larger for the magnetic reconnection considered here.

The strain rates are assumed to be

$$\alpha = -s_0, \quad \beta = s_0, \quad \gamma = 0,$$

where s_0 is a constant. The parameters are chosen as

$$a^* = \frac{a}{X_0} = 0.2, \quad \mu = \frac{B_0}{s_0 X_0} = 0.5, \quad Lu = 200, \quad Pr = 1, \quad k = 4, \\ \varepsilon = 0.5, \quad Y = 0, 0.25,$$

where $Lu = B_0 X_0 / \eta$ is the Lundquist number and $Pr = \nu / \eta$ the magnetic Prandtl number.

Fig. 10 shows the evolution of the magnetic flux in one sheet, defined by

$$\Psi_B(t) = \int_0^\infty dx B_y = \Psi_B^{(0)}(t) + \varepsilon^2 \Psi_B^{(2)}(t) + O(\varepsilon^4). \quad (31)$$

The leading-order and second-order terms are retained in the present results. The two profiles almost collapse allowing for a time-shift corresponding to the fact that the start time for reconnection depends on the initial separation of the tube sections; the profiles are similar to those obtained by Moffatt and Hunt (2002).

The evolution of the second-order flux $\Psi_B^{(2)}$ is shown in Fig. 11. Fig. 11(a) compares Ψ_B and $\Psi_B^{(2)}$. The second-order effect is small; as in vortex reconnection, the nonlinear effect is small in the integrated quantities. Fig. 11(b) shows $\Psi_B^{(2)}$ for $Y = 0$ and 0.25 . For $Y = 0$, we see that reconnection is decelerated for $1 < t < 3$ and accelerated for $t > 3$ by noting the signs of $\Psi_B^{(0)}$ and $\Psi_B^{(2)}$. This result is probably due to the Lorentz force, which acts in the $\pm x$ -direction for field lines before reconnection (Fig. 12a) so that the access to the origin, which is the point of reconnection, is delayed; it acts in the $\pm y$ -direction after reconnection (Fig. 12b). For $Y = 0.25$, however, the profile is almost reverse. This is explained as follows. Before reconnection the Lorentz force, which delays reconnection, becomes small for large Y since the curvature of magnetic lines is small. On the other hand, there is a pressure gradient drawn by dashed

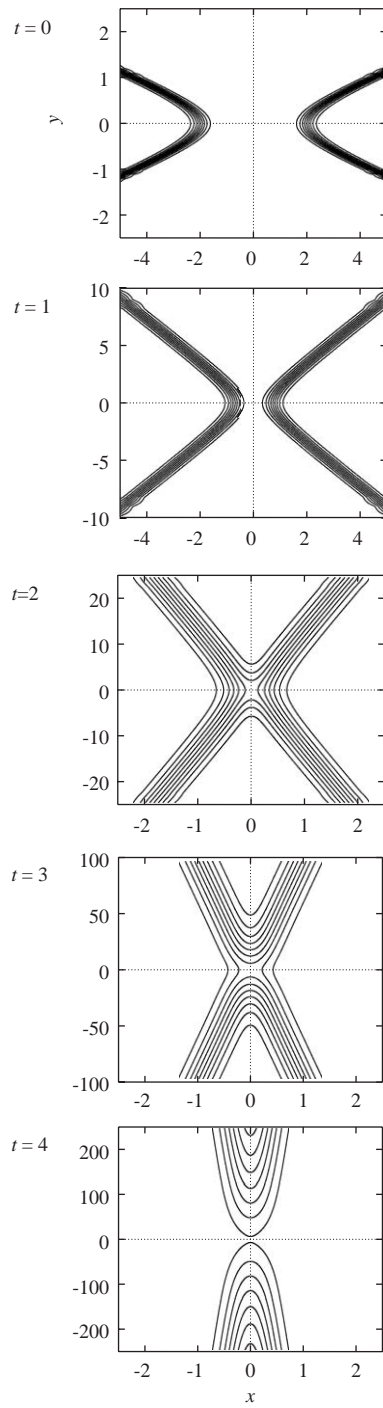


Fig. 9. Magnetic reconnection. Magnetic field lines in xy -plane. $\varepsilon = 0.5$.

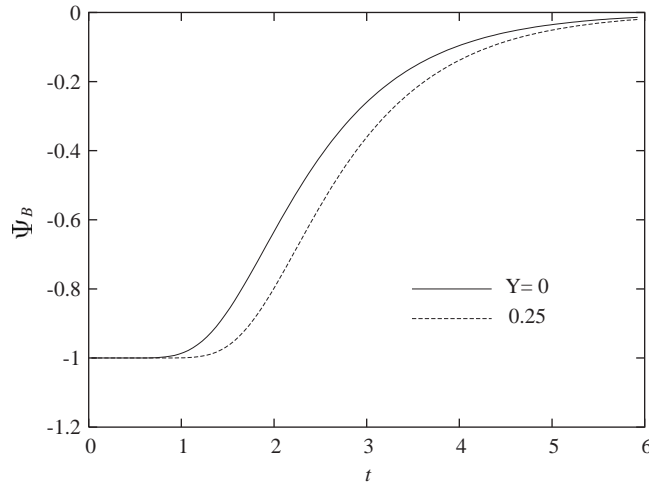


Fig. 10. Time evolution of magnetic flux of one sheet.

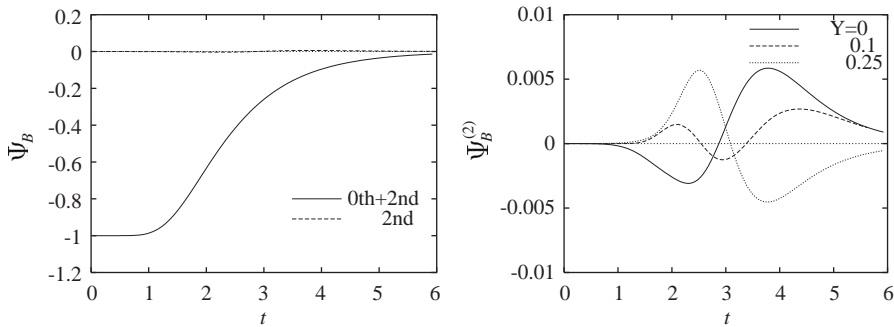


Fig. 11. Time evolution of magnetic flux of one tube. (Left) comparison between the total flux and the second-order term, (right) the second-order term at different heights: $Y = 0, 0.1$ and 0.25 .

vectors in Fig. 12(a) because of the strong Lorentz force around $Y = 0$. This pressure gradient, which accelerates reconnection, is larger than the Lorentz force for $Y = 0.25$. The situation is reversed after reconnection (Fig. 12b).

4. Concluding remarks

We have analysed vortex and magnetic reconnection of flat tubes under an imposed strain field by means of a perturbation expansion. Assuming ‘flatness’ of the tube sections, the equations of motion are reduced to one-dimensional diffusion equations at each order in ε , the ratio of axes of elliptical section at $t = 0$. Some examples show how nonlinear effects change the dynamics of reconnection which is a simple diffusion process at leading order. Although the overall effects are small, some dynamical features are captured.

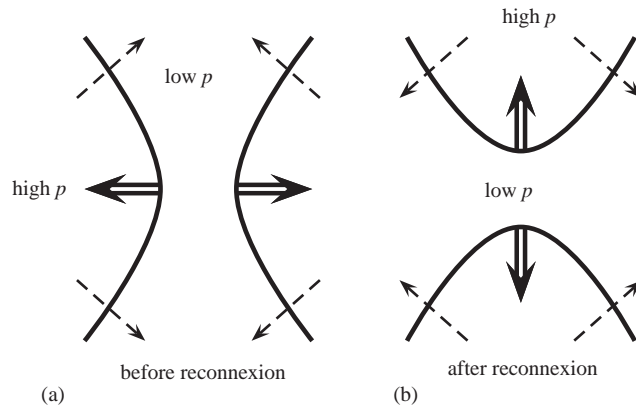


Fig. 12. Direction of Lorentz force (a) before and (b) after magnetic reconnection.

Comparing vortex and magnetic reconnection, we observe not only common properties but also differences. The leading-order motions are identical because the vorticity equation in the hydrodynamic case has the same structure as the induction equation. Since the nonlinear effects are small in the integrated quantities, the values of the reconnection rate measured by the circulation and the magnetic flux behave quite similarly. However, the nonlinear effects are different. For vortex reconnection, nonlinearity accelerates the reconnection process. This is due to a second-order effect which makes the vortex cores rotate in mutually opposite directions. For magnetic reconnection, the Lorentz force retards the reconnection process at first and accelerates it later; this is explained by the direction of the Lorentz force before and after reconnection. This is also a second-order effect. One of the sources of the differences is the direction in which field variation is of primary importance: the z -direction for vortex reconnection, and the y -direction for magnetic reconnection. Another source of the differences is the order of nonlinearity; as we have discussed in Section 3, the nonlinear terms of the vorticity equation in the hydrodynamic case are essentially second order in \mathbf{u} , while in the magnetic case the nonlinear terms of the induction equation are linear in \mathbf{B} . As a result the expansion parameter is actually ε^2 for magnetic reconnection. The dynamics is essentially two-dimensional if we ignore weak diffusion in the z -direction, as B_z vanishes up to $O(\varepsilon^3)$, whereas ω_z does not vanish at $O(\varepsilon^2)$ for vortex reconnection.

One of the advantages of the present method is that we need only solve a single set of one-dimensional diffusion equations in order to obtain field data on a two-dimensional plane. Three-dimensional data can be obtained by solving a number of sets of equations for different Y ; these are time-consuming, and we have followed this procedure only for producing Fig. 3.

Finally we comment on possible extensions of the present study. Two situations, which are more realistic, may be studied by the present technique: the case of circular cores and the case of non-parallel tubes. The spatial dimension of the resulting diffusion equations derived by perturbation expansion increases from one to two for these cases. In principle, however, the method used in the present study can be applied with appropriate modification. This provides a possible starting point for the study of unsteady reconnection, a phenomenon which still lacks sufficient understanding.

It is a privilege to dedicate this paper to the memory of Richard Pelz, a scientist of the greatest warmth and integrity, who would always generously share his thoughts and exceptional insights in problems of vortex dynamics.

This work was initiated in 2002/3 when HKM held the Chaire International de Recherche Blaise Pascal, funded by the Fondation de l'École Normale Supérieure. This support, and also that of the Leverhulme Trust, is gratefully acknowledged.

Appendix A. Equations at each order: hydrodynamic case

A.1. $O(\varepsilon^1)$

At the first order, the incompressibility condition is

$$\frac{\partial u^{(1)}}{\partial x} + \frac{\partial w^{(0)}}{\partial \tilde{z}} = 0. \quad (\text{A.1})$$

This determines $u^{(1)}$. The x -component of the vorticity equation is

$$(L_v - \alpha) \frac{\partial w^{(0)}}{\partial \tilde{y}} = 0,$$

which is consistent with (9). The y -component is

$$-(L_v - \beta) \frac{\partial w^{(1)}}{\partial x} = \left(u^{(1)} \frac{\partial}{\partial x} + w^{(0)} \frac{\partial}{\partial \tilde{z}} \right) \frac{\partial w^{(0)}}{\partial x},$$

which integrates with the aid of (A.1) to

$$(L_v + \gamma) w^{(1)} = - \left(u^{(1)} \frac{\partial}{\partial x} + w^{(0)} \frac{\partial}{\partial \tilde{z}} \right) w^{(0)}. \quad (\text{A.2})$$

Here we allow α , β and γ to be time-dependent. The z -component is

$$(L_v - \gamma) \frac{\partial v^{(1)}}{\partial x} = 0,$$

or equivalently,

$$(L_v + \beta) v^{(1)} = 0. \quad (\text{A.3})$$

Thus if, as we may assume, $v^{(1)} = 0$ at $t = 0$, then this condition persists for all $t > 0$.

A.2. $O(\varepsilon^2)$

At the second order, the incompressibility condition is

$$\frac{\partial u^{(2)}}{\partial x} + \frac{\partial v^{(1)}}{\partial \tilde{y}} + \frac{\partial w^{(1)}}{\partial \tilde{z}} = 0. \quad (\text{A.4})$$

The x -component of the vorticity equation is

$$(L_v - \alpha) \left(\frac{\partial w^{(1)}}{\partial \tilde{y}} - \frac{\partial v^{(1)}}{\partial \tilde{z}} \right) = - \left(u^{(1)} \frac{\partial}{\partial x} + w^{(0)} \frac{\partial}{\partial \tilde{z}} \right) \frac{\partial w^{(0)}}{\partial \tilde{y}} - \frac{\partial w^{(0)}}{\partial x} \frac{\partial u^{(1)}}{\partial \tilde{y}} + \frac{\partial w^{(0)}}{\partial \tilde{y}} \frac{\partial u^{(1)}}{\partial x},$$

which, when integrated, turns out to be identical with (A.2). The y -component is

$$(L_v - \beta) \left(\frac{\partial w^{(2)}}{\partial x} - \frac{\partial u^{(1)}}{\partial \tilde{z}} \right) = -u^{(1)} \frac{\partial^2 w^{(1)}}{\partial x^2} - w^{(0)} \frac{\partial^2 w^{(1)}}{\partial x \partial \tilde{z}} - u^{(2)} \frac{\partial^2 w^{(0)}}{\partial x^2} - v^{(1)} \frac{\partial^2 w^{(0)}}{\partial x \partial \tilde{y}} \\ - w^{(1)} \frac{\partial^2 w^{(0)}}{\partial x \partial \tilde{z}} - \frac{\partial w^{(0)}}{\partial x} \frac{\partial v^{(1)}}{\partial \tilde{y}} + \frac{\partial w^{(0)}}{\partial \tilde{y}} \frac{\partial v^{(1)}}{\partial \tilde{z}} + v \nabla_{\tilde{y}\tilde{z}}^2 \frac{\partial w^{(0)}}{\partial x}, \quad (\text{A.5})$$

where $\nabla_{\tilde{y}\tilde{z}}^2 = \partial_{\tilde{y}}^2 + \partial_{\tilde{z}}^2$. The z -component is

$$(L_v - \gamma) \left(\frac{\partial v^{(2)}}{\partial x} - \frac{\partial u^{(1)}}{\partial \tilde{y}} \right) = -u^{(1)} \frac{\partial^2 v^{(1)}}{\partial x^2} - w^{(0)} \frac{\partial^2 v^{(1)}}{\partial x \partial \tilde{z}} + \frac{\partial v^{(1)}}{\partial x} \frac{\partial w^{(0)}}{\partial \tilde{z}} - \frac{\partial v^{(1)}}{\partial \tilde{z}} \frac{\partial w^{(0)}}{\partial x}. \quad (\text{A.6})$$

If $v^{(1)} = 0$ then the y - and z -components become

$$(L_v - \beta) \left(\frac{\partial w^{(2)}}{\partial x} - \frac{\partial u^{(1)}}{\partial \tilde{z}} \right) = -u^{(1)} \frac{\partial^2 w^{(1)}}{\partial x^2} - w^{(0)} \frac{\partial^2 w^{(1)}}{\partial x \partial \tilde{z}} \\ - u^{(2)} \frac{\partial^2 w^{(0)}}{\partial x^2} - w^{(1)} \frac{\partial^2 w^{(0)}}{\partial x \partial \tilde{z}} + v \nabla_{\tilde{y}\tilde{z}}^2 \frac{\partial w^{(0)}}{\partial x},$$

$$(L_v - \gamma) \left(\frac{\partial v^{(2)}}{\partial x} - \frac{\partial u^{(1)}}{\partial \tilde{y}} \right) = 0,$$

or equivalently,

$$(L_v + \gamma) \left(w^{(2)} - \frac{\partial \Psi^{(1)}}{\partial \tilde{z}} \right) = -u^{(1)} \frac{\partial w^{(1)}}{\partial x} - w^{(0)} \frac{\partial w^{(1)}}{\partial \tilde{z}} - u^{(2)} \frac{\partial w^{(0)}}{\partial x} \\ - w^{(1)} \frac{\partial w^{(0)}}{\partial \tilde{z}} + v \nabla_{\tilde{y}\tilde{z}}^2 w^{(0)}, \quad (\text{A.7})$$

$$(L_v + \beta) \left(v^{(2)} - \frac{\partial \Psi^{(1)}}{\partial \tilde{y}} \right) = 0, \quad (\text{A.8})$$

where

$$\Psi^{(1)} = \int^x u^{(1)} dx. \quad (\text{A.9})$$

The incompressibility condition is

$$\frac{\partial u^{(2)}}{\partial x} + \frac{\partial w^{(1)}}{\partial \tilde{z}} = 0. \quad (\text{A.10})$$

A.3. Reduction to one-dimensional diffusion equations

We now define new coordinates (X, Y, Z) by

$$X = F_x(t; 0)x, \quad Y = F_y(t; 0)\tilde{y}, \quad Z = F_z(t; 0)\tilde{z}, \tag{A.11}$$

where

$$\begin{aligned} F_x(t; t') &= \exp \left[- \int_{t'}^t \alpha(s) ds \right], & F_y(t; t') &= \exp \left[- \int_{t'}^t \beta(s) ds \right], \\ F_z(t; t') &= \exp \left[- \int_{t'}^t \gamma(s) ds \right]. \end{aligned} \tag{A.12}$$

We also define $\hat{u}^{(i)}, \hat{v}^{(i)}, \hat{w}^{(i)}$ as

$$\hat{u}^{(i)} = [F_x(t; 0)]^{-1}u^{(i)}, \quad \hat{v}^{(i)} = [F_y(t; 0)]^{-1}v^{(i)}, \quad \hat{w}^{(i)} = [F_z(t; 0)]^{-1}w^{(i)}. \tag{A.13}$$

Then the above equations become

$$\mathcal{L}_v \hat{w}^{(0)} = 0, \tag{A.14}$$

$$\frac{\partial \hat{u}^{(1)}}{\partial X} = - \frac{\partial \hat{w}^{(0)}}{\partial Z} F_x^{-2} F_z^2, \tag{A.15}$$

$$\mathcal{L}_v \hat{w}^{(1)} = - F_x^2 \hat{u}^{(1)} \frac{\partial \hat{w}^{(0)}}{\partial X} - F_z^2 \hat{w}^{(0)} \frac{\partial \hat{w}^{(0)}}{\partial Z}, \tag{A.16}$$

$$\frac{\partial \hat{u}^{(2)}}{\partial X} = - \frac{\partial \hat{w}^{(1)}}{\partial Z} F_x^{-2} F_z^2, \tag{A.17}$$

$$\begin{aligned} \mathcal{L}_v \left(\hat{w}^{(2)} - \frac{\partial \Psi^{(1)}}{\partial Z} \right) &= - F_x^2 \hat{u}^{(1)} \frac{\partial \hat{w}^{(1)}}{\partial X} - F_z^2 \hat{w}^{(0)} \frac{\partial \hat{w}^{(1)}}{\partial Z} - F_x^2 \hat{u}^{(2)} \frac{\partial \hat{w}^{(0)}}{\partial X} \\ &\quad - F_z^2 \hat{w}^{(1)} \frac{\partial \hat{w}^{(0)}}{\partial Z} + v \mathcal{D}_{YZ} \hat{w}^{(0)}, \end{aligned} \tag{A.18}$$

$$\mathcal{L}_v \left(\hat{v}^{(2)} - \frac{\partial \Psi^{(1)}}{\partial Y} \right) = 0, \tag{A.19}$$

where

$$\mathcal{L}_v = \frac{\partial}{\partial t} - v F_x^2 \frac{\partial^2}{\partial X^2}, \quad \mathcal{D}_{YZ} = F_y^2 \frac{\partial^2}{\partial Y^2} + F_z^2 \frac{\partial^2}{\partial Z^2}. \tag{A.20}$$

We assume $\hat{w}^{(0)}$ is separable in Z at $t = 0$, i.e.

$$\hat{w}^{(0)} = \bar{w}^{(0)}(X, Y; 0)h(Z). \tag{A.21}$$

Then $\hat{w}^{(0)}$ remains separable for all t and the equations above become

$$\mathcal{L}_v \bar{w}^{(0)} = 0, \tag{A.22}$$

$$\frac{\partial^2 \bar{\Psi}^{(1)}}{\partial X^2} = \frac{\partial \bar{u}^{(1)}}{\partial X} = -\bar{w}^{(0)} F_x^{-2} F_z^2, \tag{A.23}$$

$$\mathcal{L}_v \bar{w}^{(1)} = -F_x^2 \bar{u}^{(1)} \frac{\partial \bar{w}^{(0)}}{\partial X} - F_z^2 [\bar{w}^{(0)}]^2, \tag{A.24}$$

$$\frac{\partial \bar{u}^{(2)}}{\partial X} = -\bar{w}^{(1)} F_x^{-2} F_z^2, \tag{A.25}$$

$$\mathcal{L}_v \bar{w}_m^{(2)} = \bar{s}_m, \quad m = 1, \dots, 5, \tag{A.26}$$

where \bar{f} is independent of Z and

$$\begin{aligned} \hat{u}^{(1)} &= \bar{u}^{(1)} h', & \Psi^{(1)} &= \bar{\Psi}_1 h', & \hat{w}^{(1)} &= \bar{w}^{(1)} \frac{1}{2} (h^2)', & \hat{u}^{(2)} &= \bar{u}^{(2)} \frac{1}{2} (h^2)'', \\ \hat{w}^{(2)} &= \bar{w}_1^{(2)} h (h')^2 + \bar{w}_2^{(2)} (h^2 h')' + \bar{w}_3^{(2)} \frac{1}{2} h (h^2)'' + \bar{w}_4^{(2)} h + (\bar{\Psi}^{(1)} + \bar{w}_5^{(2)}) h'', \\ \bar{s}_1 &= -F_x^2 \bar{u}^{(1)} \frac{\partial \bar{w}^{(1)}}{\partial X}, & \bar{s}_2 &= -F_z^2 \bar{w}^{(0)} \bar{w}^{(1)}, & \bar{s}_3 &= -F_x^2 \bar{u}^{(2)} \frac{\partial \bar{w}^{(0)}}{\partial X}, \\ \bar{s}_4 &= \nu F_y^2 \frac{\partial^2 \bar{w}^{(0)}}{\partial Y^2}, & \bar{s}_5 &= \nu F_z^2 \bar{w}^{(0)}. \end{aligned}$$

The one-dimensional diffusion equation

$$\mathcal{L}_v f(X, Y; t) = s(X, Y; t), \tag{A.27}$$

has solution

$$\begin{aligned} f(X, Y; t) &= \int f(X', Y; 0) G(X - X'; t, t') dX' \\ &+ \int \int s(X', Y; t') G(X - X'; t, t') dX' dt', \end{aligned} \tag{A.28}$$

where

$$G(X; t, t') = \frac{1}{\sqrt{4\pi\nu D_x(t; t')}} \exp\left[-\frac{X^2}{4\nu D_x(t; t')}\right] \tag{A.29}$$

$$D_x(t; t') = \int_{t'}^t [F_x(s; t')]^2 ds. \tag{A.30}$$

A.4. Remark on the initial conditions of the example

The example considered in (14) actually starts from $t = t_i < 0$

$$\begin{aligned} \bar{w}^{(0)}(X, Y; t_i) &= W_0 \left[H(k^2 Y^2 - X^2 + X_0^2) - \frac{1}{2} \right], \\ h(Z) &= \exp\left(-\frac{Z^2}{a^2}\right), \end{aligned} \tag{A.31}$$

where $H(\cdot)$ is the Heaviside function. Then

$$\bar{w}^{(0)}(X, Y; t) = \frac{W_0}{\sqrt{\pi}} \left[\operatorname{erf} \left(\frac{X + \sqrt{k^2 Y^2 + X_0^2}}{\sqrt{4\nu D_x(t; t_i)}} \right) - \operatorname{erf} \left(\frac{X - \sqrt{k^2 Y^2 + X_0^2}}{\sqrt{4\nu D_x(t; t_i)}} \right) - \frac{\sqrt{\pi}}{2} \right], \quad (\text{A.32})$$

and $\bar{u}^{(1)}$ and $\bar{\Psi}_1$ can be found by explicit integration. In order to avoid a singularity, we set t_i to be negative and $4\nu D_x(0; t_i) = a^2$.

Appendix B. Equations at each order: MHD case

In addition to the expansions of the velocity and magnetic fields, we expand the total pressure p_* as

$$p_* = \varepsilon^{-2} \frac{1}{2} (\beta \tilde{y}^2 + \gamma \tilde{z}^2) + \frac{1}{2} \alpha x^2 + \varepsilon p_*^{(1)} + \varepsilon^2 p_*^{(2)} + \dots,$$

where $O(\varepsilon^{-2})$ and $O(\varepsilon^0)$ terms balance the imposed strain field.

B.1. $O(\varepsilon^0)$

At the leading order, the only nontrivial equation is the y-component of the induction equation

$$(L_\eta - \beta) B_y^{(0)} = 0. \quad (\text{B.1})$$

B.2. $O(\varepsilon^1)$

At the first order, the incompressibility condition is

$$\frac{\partial u^{(1)}}{\partial x} = 0, \quad (\text{B.2})$$

which implies $u^{(1)} = 0$. Then the x- and z-components of the momentum equation are

$$0 = -\frac{\partial p_*^{(1)}}{\partial x}, \quad (\text{B.3})$$

$$(L_\nu + \gamma) w^{(1)} = 0, \quad (\text{B.4})$$

which imply

$$w^{(1)} = p_*^{(1)} = 0. \quad (\text{B.5})$$

The solenoidal condition of the magnetic field is

$$\frac{\partial B_x^{(1)}}{\partial x} = -\frac{\partial B_y^{(0)}}{\partial \tilde{y}}. \quad (\text{B.6})$$

Then the y -component of the momentum equation is

$$(L_v + \beta)v^{(1)} = B_x^{(1)} \frac{\partial B_y^{(0)}}{\partial x} - B_y^{(0)} \frac{\partial B_x^{(1)}}{\partial x}. \quad (\text{B.7})$$

The induction equation is

$$(L_\eta - \alpha)B_x^{(1)} = 0, \quad (\text{B.8})$$

$$(L_\eta - \beta)B_y^{(1)} = 0, \quad (\text{B.9})$$

$$(L_\eta - \gamma)B_z^{(1)} = 0. \quad (\text{B.10})$$

The x -component is consistent with (B.6). The other two imply $B_y^{(1)} = B_z^{(1)} = 0$.

B.3. $O(\varepsilon^2)$

At the second order, the incompressibility condition is

$$\frac{\partial u^{(2)}}{\partial x} = -\frac{\partial v^{(1)}}{\partial \tilde{y}}, \quad (\text{B.11})$$

which determines $u^{(2)}$. Then the x -component of the momentum equation is

$$\frac{\partial p_*^{(2)}}{\partial x} = -(L_v + \alpha)u^{(2)} + \frac{\partial}{\partial x} \left(\frac{1}{2} [B_x^{(1)}]^2 \right) + B_y^{(0)} \frac{\partial B_x^{(1)}}{\partial \tilde{y}}, \quad (\text{B.12})$$

which determines $p_*^{(2)}$.

The solenoidal condition of the magnetic field is

$$\frac{\partial B_x^{(2)}}{\partial x} = 0, \quad (\text{B.13})$$

which implies $B_x^{(2)} = 0$. Then the y - and z -components of the momentum equation are

$$(L_v + \beta)v^{(2)} = 0, \quad (\text{B.14})$$

$$(L_v + \gamma)w^{(2)} = 0, \quad (\text{B.15})$$

which imply $v^{(2)} = w^{(2)} = 0$.

The induction equation is now

$$(L_\eta - \beta)B_y^{(2)} = - \left(u^{(2)} \frac{\partial}{\partial x} + v^{(1)} \frac{\partial}{\partial \tilde{y}} \right) B_y^{(0)} \quad (\text{B.16})$$

$$+ \left(B_x^{(1)} \frac{\partial}{\partial x} + B_y^{(0)} \frac{\partial}{\partial \tilde{y}} \right) v^{(1)} + \eta \nabla_{\tilde{y}z}^2 B_y^{(0)}, \quad (\text{B.17})$$

$$(L_\eta - \gamma)B_z^{(2)} = 0. \quad (\text{B.18})$$

$$(\text{B.19})$$

The z -component implies $B_z^{(2)} = 0$.

B.4. Reduction to one-dimensional diffusion equations

As in the case of vortex reconnection, introducing

$$X = F_x(t; 0)x, \quad Y = F_y(t; 0)\tilde{y}, \quad Z = F_z(t; 0)\tilde{z},$$

and defining $\hat{u}^{(i)}, \hat{v}^{(i)}, \hat{w}^{(i)}$ and $\hat{B}_x^{(i)}, \hat{B}_y^{(i)}, \hat{B}_z^{(i)}$ as

$$\begin{aligned} \hat{u}^{(i)} &= [F_x(t; 0)]^{-1}u^{(i)}, & \hat{v}^{(i)} &= [F_y(t; 0)]^{-1}v^{(i)}, & \hat{w}^{(i)} &= [F_z(t; 0)]^{-1}w^{(i)}, \\ \hat{B}_x^{(i)} &= [F_x(t; 0)]B_x^{(i)}, & \hat{B}_y^{(i)} &= [F_y(t; 0)]B_y^{(i)}, & \hat{B}_z^{(i)} &= [F_z(t; 0)]B_z^{(i)}, \end{aligned}$$

we obtain the following equations in a form appropriate for numerical treatment:

$$\mathcal{L}_\eta \hat{B}_y^{(0)} = 0, \tag{B.20}$$

$$\frac{\partial \hat{B}_x^{(1)}}{\partial X} = -\frac{\partial \hat{B}_y^{(0)}}{\partial Y}, \tag{B.21}$$

$$\mathcal{L}_v \hat{v}^{(1)} = F_y^{-2} \hat{B}_x^{(1)} \frac{\partial \hat{B}_y^{(0)}}{\partial X} + F_y^{-2} \hat{B}_y^{(0)} \frac{\partial \hat{B}_y^{(0)}}{\partial Y}, \tag{B.22}$$

$$\mathcal{L}_v \frac{\partial \hat{v}^{(1)}}{\partial Y} = F_y^{-2} \hat{B}_x^{(1)} \frac{\partial^2 \hat{B}_y^{(0)}}{\partial X \partial Y} + F_y^{-2} \hat{B}_y^{(0)} \frac{\partial^2 \hat{B}_y^{(0)}}{\partial Y^2} + F_y^{-2} \frac{\partial \hat{B}_x^{(1)}}{\partial Y} \frac{\partial \hat{B}_y^{(0)}}{\partial X} + F_y^{-2} \left(\frac{\partial \hat{B}_y^{(0)}}{\partial Y} \right)^2, \tag{B.23}$$

$$\frac{\partial \hat{u}^{(2)}}{\partial X} = -\frac{\partial \hat{v}^{(1)}}{\partial Y} F_x^{-2} F_y^2, \tag{B.24}$$

$$\begin{aligned} \mathcal{L}_\eta \hat{B}_y^{(2)} &= -F_x^2 \hat{u}^{(2)} \frac{\partial \hat{B}_y^{(0)}}{\partial X} - F_y^2 \hat{v}^{(1)} \frac{\partial \hat{B}_y^{(0)}}{\partial Y} + F_y^2 \hat{B}_x^{(1)} \frac{\partial \hat{v}^{(1)}}{\partial X} \\ &\quad + F_y^2 \hat{B}_y^{(0)} \frac{\partial \hat{v}^{(1)}}{\partial Y} + \eta \mathcal{L}_{YZ} \hat{B}_y^{(0)}. \end{aligned} \tag{B.25}$$

Note that (B.23), which is the derivative of (B.22), is included in the above set in order to avoid numerical differentiation in Y ; i.e. we can regard Y as a parameter for a given set of initial conditions.

References

Bajer, K., Moffatt, H.K., 2002. *Tubes Sheets and Singularities in Fluid Dynamics*. Kluwer Academic Publishers, Dordrecht.
 Craig, I.J.D., Henton, S.M., 1995. Exact solutions for steady state incompressible magnetic reconnection. *Astrophys. J.* 450, 280–288.
 Fukumoto, Y., Moffatt, H.K., 2000. Motion and expansion of a viscous vortex ring. Part 1. A higher-order asymptotic formula for the velocity. *J. Fluid Mech.* 417, 1–45.
 Kambe, T., 1983. A class of exact solutions of two-dimensional viscous flow. *J. Phys. Soc. Japan* 52, 834–841.
 Kida, S., Takaoka, M., 1994. Vortex reconnection. *Annu. Rev. Fluid Mech.* 26, 169–189.
 Lele, S.K., 1992. Compact finite-difference schemes with spectral-like resolution. *J. Comp. Phys.* 103, 16–42.
 Melander, M.V., Hussain, F., 1988. Cut-and-connect of two antiparallel vortex tubes. Center for Turbulence Research Proc. Summer Program.

- Moffatt, H.K., 1978. *Magnetic Field Generation in Electrically Conducting Fluids*. Cambridge University Press, Cambridge, pp. 50–51.
- Moffatt, H.K., Hunt, R.E., 2002. A model for magnetic reconnection. In: Bajer, K., Moffatt, H.K. (Eds.), *Tubes Sheets and Singularities in Fluid Dynamics*. Kluwer Academic Publishers, Dordrecht, pp. 125–132.
- Pelz, R.B., 1997. Locally self-similar, finite-time collapse in a high-symmetry vortex filament model. *Phys. Rev. E* 55, 1617–1620.
- Pelz, R.B., 2001. Symmetry and the hydrodynamic blowup problem. *J. Fluid Mech.* 444, 299–320.
- Priest, E.R., Forbes, T., 2000. *Magnetic Reconnection*. Cambridge University Press, Cambridge, UK.
- Priest, E.R., Titov, V.S., Grundy, R.E., Hood, A.W., 2000. Exact solutions for reconnective magnetic annihilation. *Proc. R. Soc. Lond. A* 456, 1821–1849.
- Takaoka, M., 1991. Straining effects and vortex reconnection of solutions to the 3-D Navier–Stokes equation. *J. Phys. Soc. Japan* 60, 2602–2612.